JACS Au
AN OPEN ACCESS JOURNAL OF THE AMERICAN CHEMICAL SOCIETY

pubs.acs.org/jacsau
Article

Highly Sensitive Labeling, Clickable Functionalization, and Glycoengineering of the MUC1 Neighboring System

Gang Wang,[⊥] Ying Chen,[⊥] Yuan Wei, Lei Zheng, Jianwei Jiao,* and Yuna Guo*

Cite This: *JACS Au* 2024, 4, 828−836

Read Online

ACCESS | Metrics & More | Article Recommendations | Supporting Information

ABSTRACT: This study introduces a novel wash-type affinity-primed proximity labeling (WAPL) strategy for labeling and surface engineering of the MUC1 protein neighboring system. The strategy entails the utilization of peroxidase in conjunction with a MUC1-selective aptamer, facilitating targeted binding to MUC1 and inducing covalent labeling of the protein neighboring system. This study reveals a novel finding that the WAPL strategy demonstrates superior labeling efficiency in comparison to nonwash-type affinity-primed proximity labeling, marking the first instance of such observations. The WAPL strategy provides signal amplification by converting a single recognition event into multiple covalent labeling events, thereby improving the detection sensitivity for subtle changes in MUC1. The WAPL platform employs two levels of labeling upgrades, modifying the biotin handles of the conventional labeling substrate, biotin−phenol. The first level involves a range of clickable molecules, facilitating dibenzoazacyclooctynylation, alkynylation, and *trans*-cyclooctenylation of the protein neighboring system. The second level utilizes lactose as a post-translational modification model, enabling rapid and reliable glycoengineering of the MUC1 neighboring system while remaining compatible with cell-based assays. The implementation of the WAPL strategy in protein neighboring systems has resulted in the establishment of a versatile platform that can effectively facilitate diverse monitoring and regulation techniques. This platform offers valuable insights into the regulation of relevant signaling pathways and promotes the advancement of novel therapeutic approaches, thereby bringing substantial implications for human health.

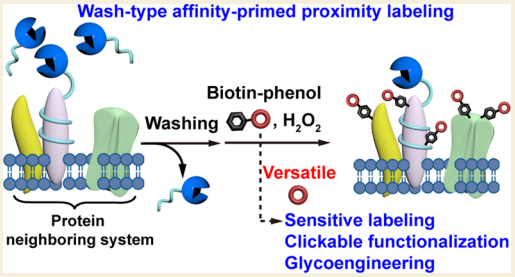

KEYWORDS: *HRP, aptamer, proximity labeling, click reaction, glycosylation*

INTRODUCTION

The spatial configuration of biomolecules is pivotal for fundamental biological processes.[1] Mucin1 (MUC1), characterized by its glycosylated structure and variable tandem repeat (VNTR) domains, exhibits an augmented expression in diverse epithelial cancers.[2,3] This protein is recognized as a critical biomarker in several cancer types, playing an integral role in disease progression and often correlating with adverse prognostic outcomes.[4] The activity and localization of MUC1 are governed by numerous molecular mechanisms including interactions with other proteins. Recent research has demonstrated that disrupting MUC1−EGFR interactions effectively eliminates breast cancer cells both *in vitro* and in tumor models.[5] Functionalizing the neighboring system of MUC1 can provide insights into the regulation of signaling pathways associated with MUC1 and aid in the development of novel therapeutic drugs.

In the study of MUC1, various classical and traditional detection methods, such as enzyme-linked immunosorbent assay (ELISA),[6] Western blot (WB),[7] mass spectrometry (MS),[8] and immunofluorescence (IF),[9] have been employed. While ELISA, WB, and MS techniques offer quantitative protein information, they often necessitate sample lysis and can be detrimental to cells, thereby limiting their ability to conduct *in situ* analysis.[10] The IF technique is a robust immunochemical method that enables the detection of various membrane proteins through the utilization of fluorophore-modified antibodies *in situ*.[11,12] While this technique can be applied to living cells to some extent, there is a need for enhanced sensitivity. Duplexed luminescence resonance energy transfer (D-LRET)[13] and hierarchical coding (HieCo)[14] strategies have made use of the highly expressed glycosyl groups on MUC1 to achieve the amplification analysis of MUC1 at the living cell level but still lack the technology to regulate protein function. Regulation of protein function often requires the rapid incorporation of functional groups into protein neighboring systems. The 2022 Nobel Prize in Chemistry recognized the significant contributions of click chemistry, which locally introduces chemical modifications such as Cu(I)-catalyzed azide−alkyne cycloaddition (CuAAC) by Sharpless and Meldal,[15] and the strain-promoted alkyne−azide cyclo-

Received: December 18, 2023
Revised: January 25, 2024
Accepted: January 25, 2024
Published: February 8, 2024

https://doi.org/10.1021/jacsau.3c00803
JACS Au 2024, 4, 828−836

Scheme 1. (A) Schematic illustrating the labeling principle of wash-type affinity-primed proximity labeling (WAPL). (B) Schematic diagram illustrating multiple functionalizations in the protein neighboring system using WAPL strategy[a]

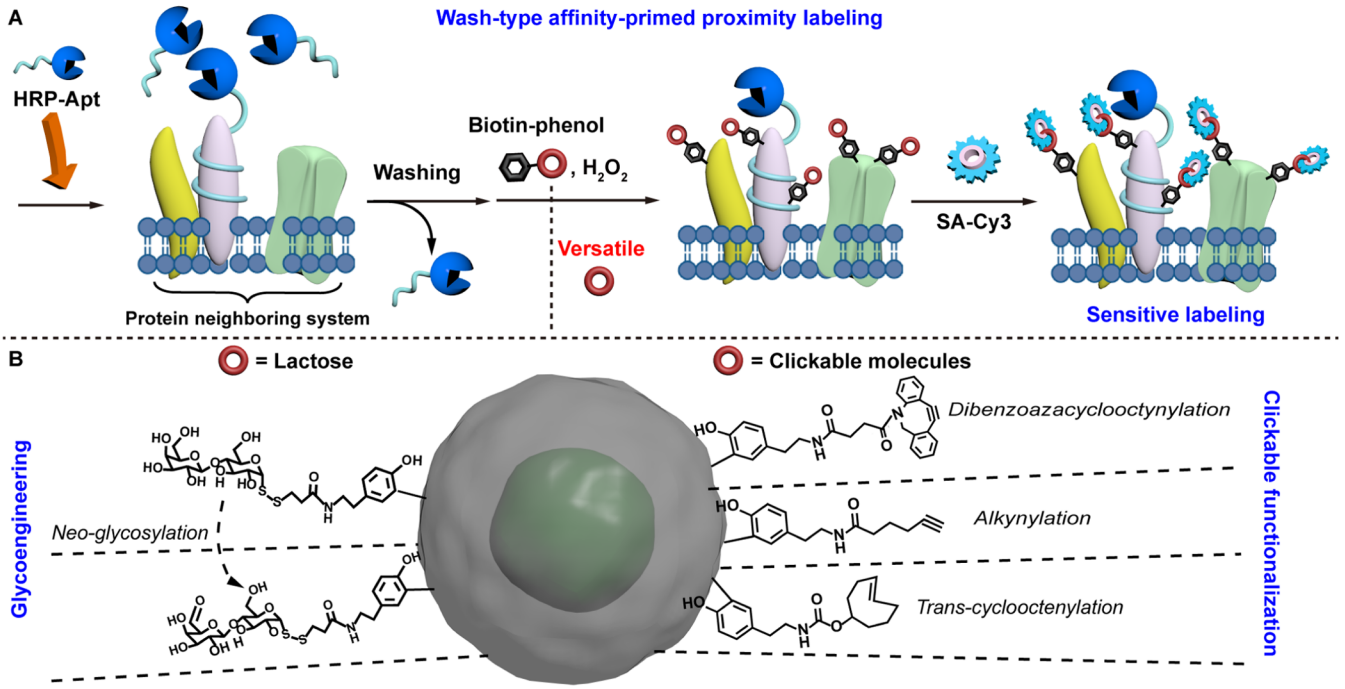

[a]The labeling results comprise two primary categories: (1) Functionalization with clickable molecules to achieve dibenzoazacyclooctynylation, alkynylation, and trans-cyclooctenylation of the proteins in the neighboring system. (2) Use of lactose as a model for post-translational modifications (PTMs) to enable rapid, reliable, and cell-compatible glycoengineering in the protein neighboring system.

addition (SPAAC) reaction by Bertozzi.[16] This integration into the protein neighboring system allows for the construction of a flexible and versatile platform that can accommodate various monitoring and regulation techniques.[17] However, the challenge lies in developing methods to locally introduce the aforementioned chemical modifications into protein neighboring systems.

Peroxidase-mediated proximity labeling provides an opportunity to address this problem.[18] In the presence of hydrogen peroxide, peroxidases catalyze the generation of phenoxy radicals from phenol derivatives. These radicals have short lifetimes (<1 ms), small labeling ranges (<20 nm), and can covalently react with electron-rich amino acids such as tyrosine, which can quickly achieve the labeling of proteins and neighboring proteins.[19,20] Peroxidase-mediated proximity labeling involves the localization of peroxidase and proximity labeling. The receptor−ligand recognition method provides a promising solution for the rapid and direct precise localization of peroxidase.[21] In all the affinity molecules, aptamer (Apt) is an oligonucleotide fragment obtained from a nucleic acid molecular library by systematic evolution of ligands by exponential enrichment (SELEX), and it is smaller and more stable than antibodies.[22,23] It has high specificity for target molecules and can be produced quickly by chemical synthesis or *in vitro* selection.[24] Furthermore, based on whether the undetermined peroxidase was washed off when approaching the label, wash-type strategies, represented by the enzyme-mediated activation of radical source (EMARS)[21] and multifunctional proximity labeling (MPL) strategy, and nonwash-type approach, represented by the aptamer-enabled proximity catalytic labeling (APCL) strategy,[26] were developed. Compared with wash-type strategies, the nonwash-type strategy is relatively simple to operate. However, the issue of possible substrate waste, resulting in compromised label validity, has not been systematically explored.

Here, we contrasted the labeling differences between nonwash-type and wash-type affinity-primed proximity labeling (WAPL) for the first time and further achieved multiple labeling and functionalization of MUC1 protein neighboring systems (Scheme 1). We selected MUC1 S2.2 Apt,[27] known for its high affinity for MUC1, as the affinity molecule and incorporated it as a spatial control for horseradish peroxidase (HRP). Then, we used molecular toolboxes to facilitate the diverse functionalization of protein neighboring systems. This allows for subsequent tracking or modification using CuAAC, SPAAC, and iEDDA reactions. All three labeling methods can be conducted *in situ* and offer remarkable selectivity and sensitivity. By employing lactose as a model, we have achieved a novel neo-glycosylation of the MUC1 neighboring system, which occurs at electron-rich amino acids different from *N*-glycosylation (asparagine) and *O*-glycosylation (serine, threonine), which has important implications for the regulation and study of glycosylation-related signaling pathways. The clickable labeling platform we constructed offers a highly efficient, cost-effective, and dependable method for incorporating drugs and other compounds into protein neighboring systems. This study provides valuable insights into the regulation of glycosylation-related signaling pathways in protein neighboring systems and the development of novel therapeutic drugs, with far-reaching implications for human health and treatment strategies.

The HRP-Apt conjugate was generated by using a stepwise assembly protocol. A bifunctional linker, 4-(*N*-maleimidomethyl) cyclohexane-1-carboxylic acid 3-sulfo-*N*-hydroxysuccinimide ester (SMCC),[28] was employed, with *N*-hydroxysucci-

https://doi.org/10.1021/jacsau.3c00803
JACS Au 2024, 4, 828−836

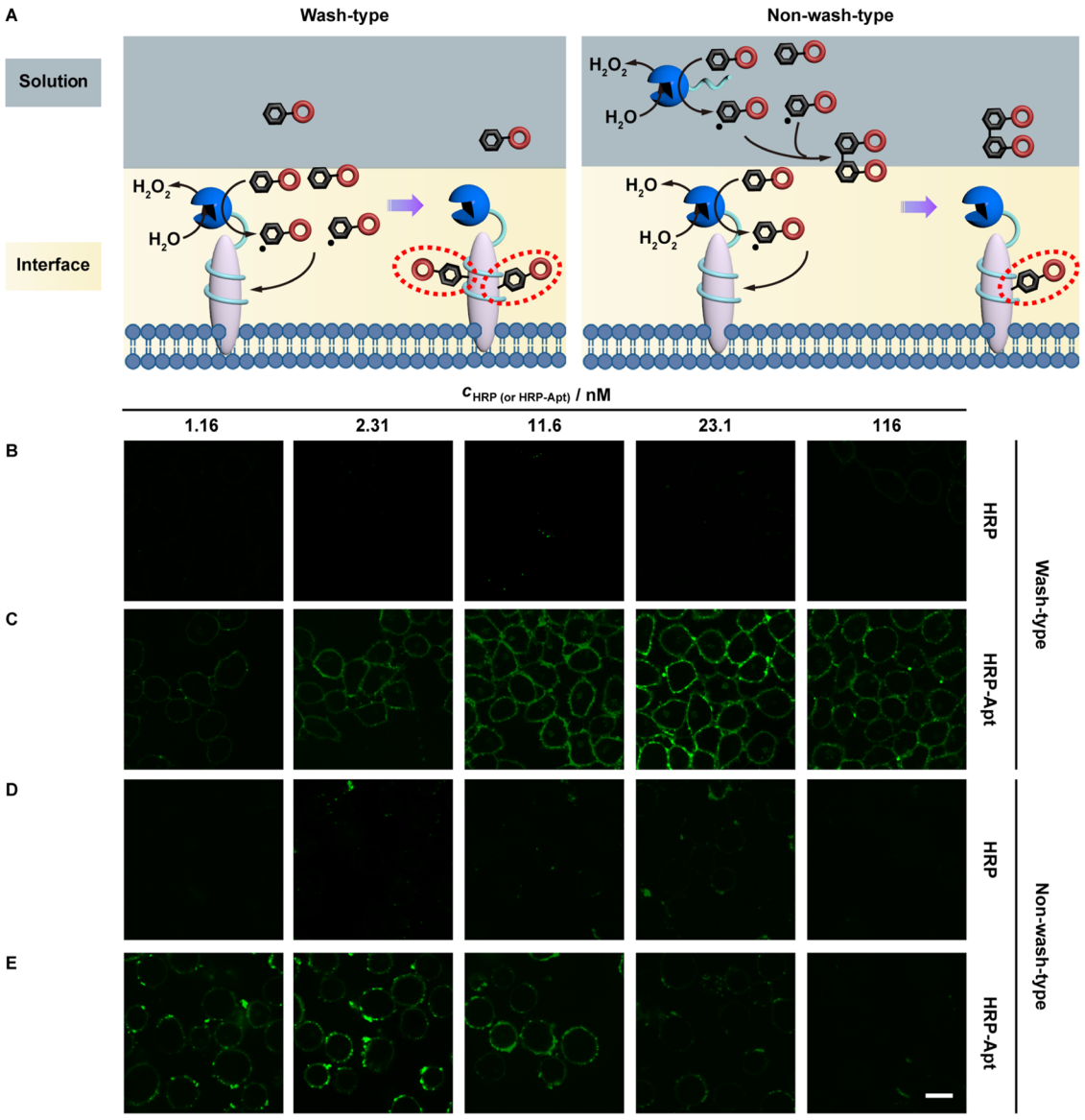

Figure 1. Differences in procedures, principles, and results between wash-type and nonwash-type affinity-primed proximity labeling. (A) Schematic illustration for the principle of the labeling. (B−E) Investigation of the labeling performance of HRP (B, D) and HRP-Apt (C, E) on wash-type (B, C) and nonwash-type (D, E) affinity-primed proximity labeling. CLSM was obtained by SA-Cy3 staining after affinity-primed proximity labeling. Scale bar: 20 μm. The images are representative of three individual experiments.

nimide (NHS) and maleimide (Mal) as its functional groups. Briefly, the surface-exposed amino groups of HRP reacted with the NHS of SMCC, resulting in the formation of HRP-SMCC. The exposed Mal on HRP-SMCC subsequently reacted with the thiol group from SH-Apt, generating HRP-Apt. The conjugation of HRP and Apt was evaluated using sodium dodecyl sulfate-polyacrylamide gel electrophoresis (SDS-PAGE) (Figure S1). The results displayed a distinct upward-shifted discrete band at 94.2% for HRP-Apt compared to HRP, indicating successful and efficient covalent coupling of HRP and Apt. HRP-Apt exhibited two additional upward-shifted bands compared with HRP, suggesting the formation of two different proportions of HRP-Apt conjugates. Subsequently, a conventional 3,3′,5,5′-tetramethylbenzidine (TMB)-based colorimetric assay was employed to validate the sustained HRP activity within the HRP-Apt conjugate (Figure S2).[29]

Having successfully prepared HRP-Apt, we proceeded to investigate the characteristics of affinity-primed proximity labeling by employing HRP-Apt. Biotin−phenol is a commonly used labeling molecule in such reactions to demonstrate the local labeling effect. Researchers have employed different approaches in the biotin−phenol labeling step, with some opting to remove unbound HRP in a process known as wash-type,[21,25] while others choose not to remove it, referred to as nonwash-type.[26] However, the efficiency of labeling in wash-type and nonwash-type affinity-primed proximity labeling has not been thoroughly examined in prior studies. To address this, MCF-7 cells were labeled with gradient concentrations of HRP and HRP-Apt under wash and nonwash conditions, as depicted in Figure 1B−E. The procedure involved incubating MCF-7 cells with HRP and HRP-Apt for 30 min. Subsequently, biotin−phenol (100 μM) and H_2O_2 (400 μM) were added under wash and no-wash conditions, followed by a 3 min incubation to accomplish labeling. Postreaction quenching and washing to eliminate excess biotin−phenol were conducted, and streptavidin-Cy3 (SA-Cy3) was utilized

https://doi.org/10.1021/jacsau.3c00803
JACS Au 2024, 4, 828−836

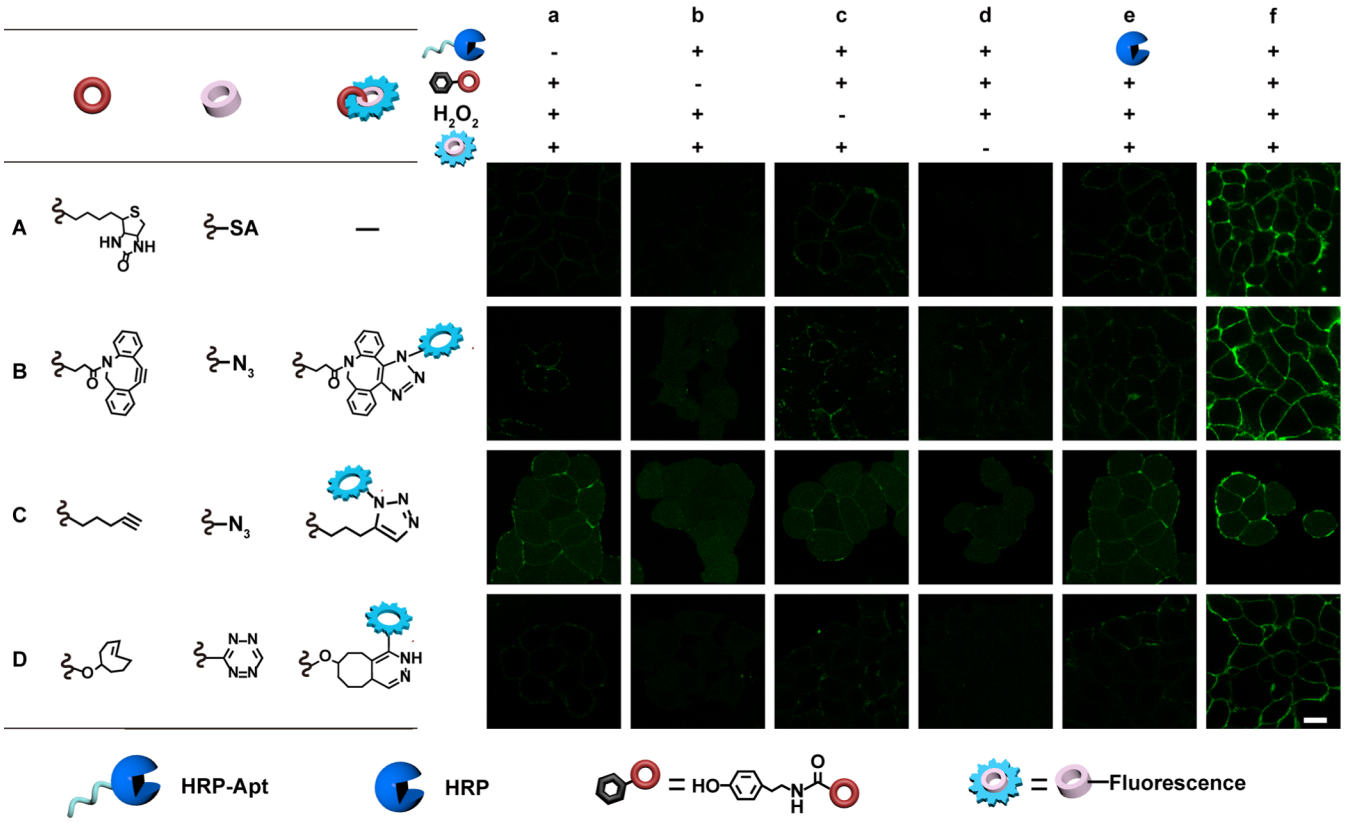

Figure 2. Demonstration of the feasibility of different phenol-modified functional molecules in the WAPL strategy. Scale bar: 20 μm. Fluorescence image: Cy3 excitation, 540 nm/emission 555−610 nm. Cy5 excitation 650 nm/emission 675−720 nm. Pictures are representative of three separate experiments.

to detect the presence of the labeled biotin−phenol (Figure 1). Notably, MCF-7 cells in the wash-type group exhibited more pronounced Cy3 fluorescence on the cell membrane than those in the nonwash-type group (Figure 1B−E). Moreover, replacing HRP-Apt with HRP resulted in significantly weaker fluorescence (Figure 1B,D). The signal ratio of HRP-Apt to HRP in the optimal case for wash-type reached 13.2 ($c_{\text{HRP-Apt}}$, 23.1 nM), whereas for nonwash-type, it was 7.8 ($c_{\text{HRP-Apt}}$, 2.31 nM) (Figures 1B−E and S3). This outcome may be attributed to the higher efficiency of the wash-type in facilitating the reaction of peroxidase-catalyzed phenoxy derivatives with electron-rich amino acids on the cell surface, whereas the nonwash-type predominantly dimerizes phenol derivatives, impeding labeling on the cell surface (Figure 1A). In short, we compared the wash-type and nonwash-type method, and the wash-type method reduces the synthesis of dimers, improves the labeling efficiency, and is very friendly to the adherent cells. The nonwash-type method is more suitable for suspension cells (Table S1). Consequently, the WAPL strategy was selected for subsequent experiments. Control experiments were conducted to validate the specificity of the WAPL strategy, where the absence of HRP-Apt, biotin−phenol, H_2O_2, or SA-Cy3 resulted in indistinguishable fluorescence intensity (FI) from the blank control. The replacement of HRP with HRP-Apt yielded no signal, confirming the localization of labeling mediated by Apt (Figures 2A and S4). The results showed that the labeling reagents exhibited favorable cytocompatibility and the cells retained their viability after WAPL. Therefore, WAPL is considered a suitable method for performing live cell experiments, as shown in Figure S5. Additionally, this study showcases the extensive versatility of the WAPL method in labeling *N*-glycosylated proteins, with EpCAM serving as a representative model (Figure S6).

Clickable functionalization of the cell surface plays a pivotal role in various aspects, including cell type identification, regulation of cell adhesion, control of cell−cell interactions, and promotion of cell apoptosis.[30−33] Localized functionalization within protein neighboring systems offers convenience for the precise regulation of cellular behavior. To facilitate manual manipulation of protein neighboring systems, we constructed a molecular toolbox. Alongside biotin−phenol (Figures 2A and S4), the toolbox included dibenzoazacyclooctyne (DBCO)−phenol (Figures 2B and S7), alkyne−phenol (Figures 2C and S8), and *trans*-cyclooctene (TCO)−phenol (Figures 2D and S9) as labeling molecules. Each molecule in the toolbox underwent conceptual verification to fully explore its labeling properties, yielding consistent results with biotin−phenol. Furthermore, our labeling technique demonstrated efficiency and rapidity, with the entire protocol taking only 33 min (30 min for Apt binding and 3 min for localized labeling), which is significantly shorter than the approximately 72 h required for endogenous expression-based approaches.

Additionally, we investigated the principles and patterns of labeling molecules in the toolbox for WAPL strategies (Figure 3A). It was observed that the fluorescence on the cells increased initially and then decreased as the concentration of the labeling molecules increased (Figures 3B and S10). When the concentration of the labeling molecules was very low, such as 1 μM, the fluorescence signal on the cells was weak due to an insufficient abundance of the labeling molecules. However,

https://doi.org/10.1021/jacsau.3c00803
JACS Au 2024, 4, 828−836

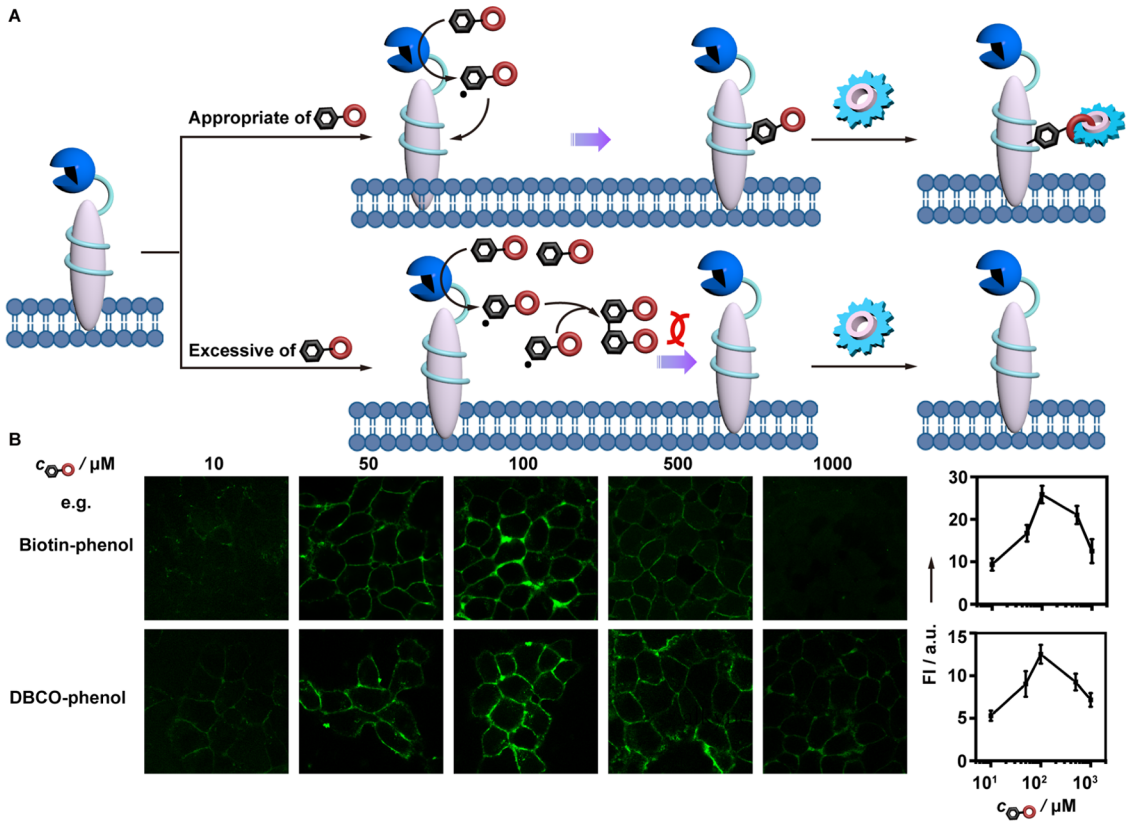

Figure 3. Effect of different concentrations of phenol-modified functional molecules on the efficacy of the WAPL strategy. (A) Illustration of labeling efficiency for different molecular concentrations in the WAPL strategy. (B) Fluorescence images and FI of biotin−phenol, DBCO−phenol at different concentrations. Representative images from three independent experiments are presented, with a scale bar indicating 20 μm.

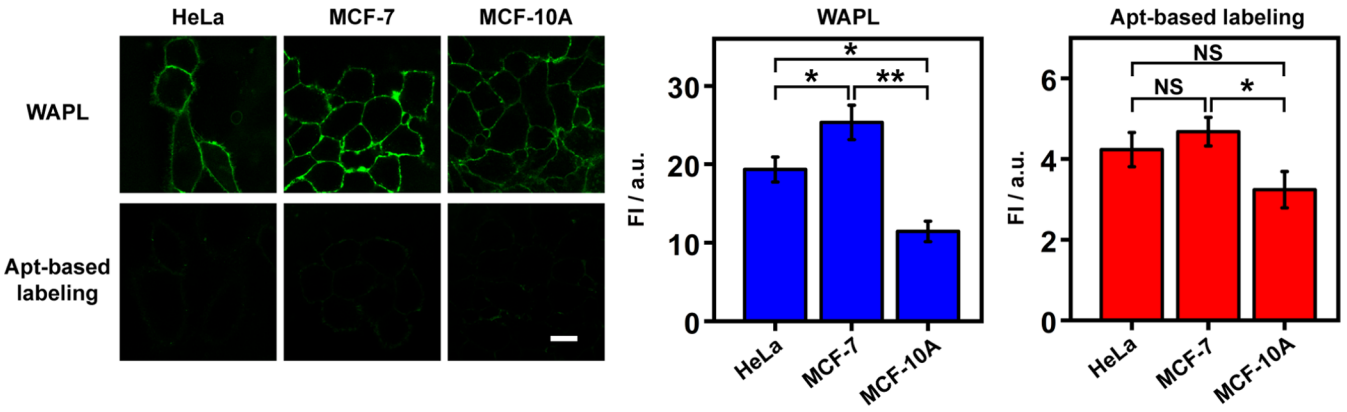

Figure 4. MUC1 expression levels in different cell types were determined by the WAPL strategy and direct Cy3-Apt labeling. HeLa, MCF-7, and MCF-10A cells were utilizing biotin−phenol as the labeling substrate, while SA-Cy3 was employed to quantify the extent of biotinylation. The fluorescence statistics for Apt-based labeling are from Figure S11. Representative images from three independent experiments are shown. Fluorescence imaging was conducted with Cy3 excitation at 540 nm and emission within the range of 555−610 nm. Scale bar: 20 μm. Data are presented as mean ± SD, $n = 3$. Statistical analysis was performed using Student's t-test, where $^{**}p < 0.01$ was considered highly significant, $^{*}0.001 < p < 0.05$ was considered significant, and $p \geq 0.05$ was regarded as not significant (NS).

the phenomenon of decreased fluorescence in cells with increasing concentrations of the labeling molecules was not commonly observed. This behavior can be attributed to the competitive nature of the labeling reaction. The peroxidase-catalyzed labeling of phenol derivatives involves competition between the phenol derivatives in the solution and the electron-rich amino acids on the cell membrane.[18−20] When the concentration of phenol radicals is appropriate, the radicals diffuse to the cell surface and react with electron-rich amino acids. However, when the concentration of phenol radicals is too high, dimerization of the phenol derivatives becomes dominant, which hinders labeling on the cell surface. The experimental observations during cell incubation with HRP-Apt (Figure 1C,E) at gradient concentrations aligned with the trends observed with the molecules in the toolbox, further confirming the competitive nature of the reactions in the WAPL strategy.

For the detection of subtle changes in MUC1, a marker for tumor occurrence, development, and prognosis, more sensitive detection methods are needed.[34] Antibody/Apt recognition is

https://doi.org/10.1021/jacsau.3c00803
JACS Au 2024, 4, 828−836

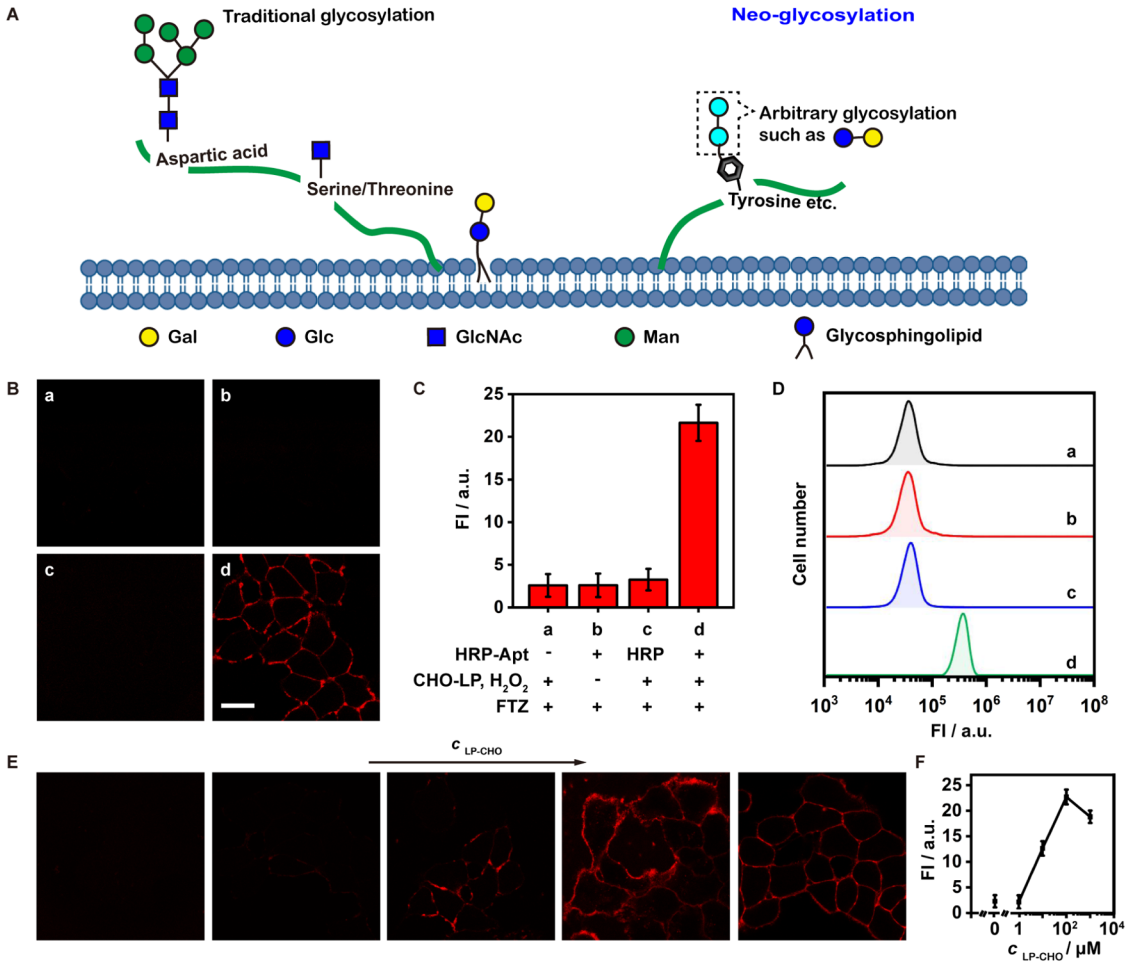

Figure 5. WAPL strategy-based neo-glycosylation of the MUC1 neighboring system in living cells. (A) Schematic illustrating the site differences between neo-glycosylation of the labeling and conventional glycosylation. (B) CLSM imaging of MCF-7 cells treated with different combinations of labeling strategies. (C) Statistical analysis of FTZ signal intensity in (B). (D) Flow cytometry (FCM) of MCF-7 cells treated with different combinations of labeling strategies. (E) Fluorescence imaging of different samples at different concentrations of LP-CHO. (F) FI of LP-CHO from (D). Scale bar: 20 μm. Fluorescence image: FITC excitation 488 nm/emission 510−550 nm. Pictures are representative of three separate experiments.

a widely used protein analysis technique that does not necessitate genetic manipulation of the target cell population.[35] Cy3-labeled aptamer (Cy3-Apt) was utilized to assess the capability of Apt-based labeling and the WAPL strategy for discriminating protein abundance in various cell lines (Figures 4 and S11). Under identical recording conditions of confocal laser scanning microscopy (CLSM), the WAPL strategy facilitated clear observation of Cy3 signals of MUC1, while the Apt-based labeling method encountered difficulties in detecting signals from certain MUC1-expressing cells. This disparity arises because the WAPL strategy amplifies a single identification event into multiple covalently labeled events, thereby producing stronger signals compared to those of the Apt-based labeling (Figure 4). Furthermore, despite enhancements in the imaging parameters of the Apt-based identification method, it often struggled to distinguish MUC1-expressing tumor cells such as MCF-7 and HeLa cells (Figure S11). In contrast, the WAPL strategy successfully identified differences and exhibited significant distinctions with these cells (Figure 4). While the Apt-based labeling approach was unable to track the difference in MUC1 abundance between MCF-7 and MCF-10A cells, the WAPL strategy was able to recognize the difference between them and showed a significant difference. This enhancement arises from the conversion of a single recognition event into multiple covalent labeling events, facilitating the detection of subtle changes in MUC1. The protein expression discrepancies observed among the three cells using the WAPL strategy were found to be in agreement with the WB results (Figure S12), suggesting that the developed WAPL strategy exhibits a high level of accuracy and sensitivity as an *in situ* analysis approach.

Glycosylation, a nontemplate-driven biological synthesis process, represents the most intricate and diverse class of modifications in cellular structures. It plays a crucial role in cell recognition, communication, adhesion, and immune response.[36,37] The advancement of swift and reliable *in situ* (neo)glycosylation on protein neighboring systems is essential for an in-depth understanding and accurate control of glycan functionality, particularly in tumor immunotherapy. To illustrate the efficacy of the WAPL strategy in addressing this challenge, lactose was employed as a glycan model to exhibit a successful glycosylation implementation (Figure 5). Lactose, comprising glucose and galactose, undergoes transformation by galactose oxidase, which converts the hydroxyl group at the C_6 position of galactose into an aldehyde group.[38] In this approach, the synthesized aldehyde lactose−phenol (CHO−

https://doi.org/10.1021/jacsau.3c00803
JACS Au 2024, 4, 828−836

LP) serves as a substrate for the WAPL strategy. The aldehyde group is bioorthogonal tagged with fluorescein-5-thiosemicarbazone (FTZ) to visualize the abundance of CHO−LP on cell membranes. CHO−LP was efficiently attached to the protein neighboring system following 3 min of proximity labeling. The contribution of each probe component was evaluated by excluding specific relevant components and replicating the protocol (Figures 5B−D and S13). The FI at the cell periphery was negligible in the absence of HRP-Apt (a), CHO−LP, H_2O_2 (b), or FTZ (c). When Apt was omitted and HRP was used to incubate the cells (d), the FI at the cell periphery was nearly the same as that of the background, indicating that the targeting effect of Apt enabled glycosylation of the MUC1 neighboring system. The localized installation principles of CHO−LP were examined, adhering to similar patterns as those observed with clickable molecules in the toolbox (Figure 5E,F). Significantly, endogenous cellular glycosylation is unaffected during neo-glycosylation, as demonstrated by sialic acid (Figure S14). The neo-glycosylation sites in the MUC1 neighboring system differ from traditional glycosylation sites, which typically involve asparagine-linked (*N*-linked) and serine/threonine-linked (*O*-linked) types. Instead, the neo-glycosylation sites are predominantly situated on electron-rich amino acids, such as tyrosine (Figure 5A). This distinction is critical for regulating and investigating signaling pathways associated with atypical glycosylation sites. Additionally, to determine the activity of glycosyl molecules incorporated during the neo-glycosylation process, a global oxidation of cellular galactose was performed following proximity labeling with lactose−phenol as the substrate. Subsequently, the oxidized galactose was tagged with FTZ (Figure S15). The notably enhanced fluorescence observed at the cell surface suggested successful incorporation and subsequent oxidation of lactose. Furthermore, an investigation into the labeling regularity of lactose−phenol revealed consistency with CHO−LP, possibly linked to substrate dimerization (Figure S16). This method is fast, user-friendly, and compatible with live cells and does not require prior chemical modification or genetic intervention of the cells, offering opportunities to study glycosylation-mediated interactions, signal transduction, and the regulation of tumor immunotherapy.

CONCLUSIONS

This research has led the way in comparing nonwash-type and wash-type affinity-primed proximity labeling. By employing this WAPL strategy, we transformed a single aptamer recognition event into multiple covalent labels facilitated by ultrafast enzyme catalysis, facilitating the observation of subtle changes in MUC1. Selective customization of various clickable groups in the MUC1 protein neighboring system has been enabled. This platform can accommodate CuAAC, SPAAC, and iEDDA reactions for subsequent tracking or modification. Significantly, we present a prompt glycosylation technique that specifically targets nonclassical sites within the adjacent protein system, thereby enabling the integration of neo-glycosylation into the MUC1 neighboring system. This approach provides opportunities for investigating the functional implications of novel glycosylation at nonnatural sites. We firmly believe that our proposed method will significantly contribute to the investigation of MUC1-related signal transduction and cellular behavior and hold substantial potential for applications in chemotherapy, immunotherapy, and tissue engineering.

METHODS

WAPL of Biotin−Phenol

MCF-7 cells were seeded at a density of 2×10^5 mL^{-1} in confocal dishes and incubated at 37 °C with 5% CO_2 for 24 h. Cells were blocked with 10% goat serum for 1 h at 4 °C and washed three times with PBS. To investigate the differences in HRP-Apt-mediated cell labeling at different concentrations, 1.16, 2.31, 11.6, 23.1, and 116 nM HRP-Apt were added to MCF-7 cell samples, incubated at 4 °C for 30 min, and washed three times with PBS. 100 μL portion of PBS solution containing 100 μM biotin−phenol and 400 μM H_2O_2 was added to the cells and maintained for 3 min. Then, 5 μL of PBS containing 200 mM NaN_3 and 200 mM sodium ascorbate was added to the reaction solution to quench the reaction, and the cells were washed three times with PBS to complete the biotin−phenol labeling process. 100 μL of 15 μg mL^{-1} of SA-Cy3 was added to the cell samples, incubated for 30 min at 4 °C, and washed three times with PBS. Finally, the fluorescence intensity (FI) of the cell surface was measured by CLSM, and the pixel values of 10 cell profiles were averaged and repeated three times to obtain the FI. To demonstrate the necessity of each component for WAPL, the labeling experiments were performed by the same procedure as mentioned above with $c_{\text{HRP-Apt}}$ of 23.1 nM except for omitting each component individually. To investigate the effect of biotin−phenol concentration ($c_{\text{biotin−phenol}}$) on WAPL performance, after cells were incubated with 23.1 nM HRP-Apt, 100 μL of PBS containing 400 μM H_2O_2 and different $c_{\text{biotin−phenol}}$ (10, 50, 100, 500, and 1000 μM) were added. Quenching was performed by adding 5 μL of PBS containing 200 mM NaN_3 and 200 mM sodium ascorbate.

Performance of the WAPL Strategy on Different Cells

MCF-7, MCF-10A, and HeLa cells were seeded at a density of 2×10^5 mL^{-1} in confocal disks and cultured at 37 °C and 5% CO_2 for 24 h. The cells were blocked with 10% goat serum at 4 °C for 1 h and washed three times with PBS. To investigate the differences in HRP-Apt-mediated labeling in cells with different MUC1 expression, 100 μL of 23.1 nM HRP-Apt was added to MCF-7, MCF-10A, and HeLa cell samples, incubated for 30 min at 4 °C, and washed three times with PBS. 100 μL of PBS solution containing 100 μM biotin−phenol and 400 μM H_2O_2 was added to the cells and maintained for 3 min. Then, 5 μL of PBS containing 200 mM NaN_3 and 200 mM sodium ascorbate was added to the reaction solution to quench the reaction, and the cells were washed three times with PBS. 100 μL of 15 μg mL^{-1} SA-Cy3 was added to the cell samples, incubated at 4 °C for 30 min, and washed three times with PBS. Finally, the FI on the cell surface was measured using CLSM. The pixel values of 10 cell profiles were averaged, and this process was repeated three times.

Cell Neo-Glycosylation by WAPL of CHO-Lactose−Phenol

MCF-7 cells were seeded at a density of 2×10^5 mL^{-1} in confocal dishes and incubated at 37 °C with 5% CO_2 for 24 h. 10% goat serum was added to the cells to block the cells at 4 °C for 1 h, followed by three washes with PBS. 100 μL portion of 23.1 nM HRP-Apt was added to MCF-7 cell samples and incubated for 30 min at 4 °C. 100 μL of PBS solution containing 100 μM CHO-lactose−phenol and 400 μM H_2O_2 was added to the cells and maintained for 3 min. Then, 5 μL of PBS containing 200 mM NaN_3 and 200 mM sodium ascorbate was added to the reaction solution to quench the reaction. After washing three times with PBS, a PBS solution containing 100 μM FTZ, 10 mM aniline, and 5% FBS (100 μL) was added to the cell samples and incubated at 4 °C for 1 h. After washing, the fluorescence on the cell surface was imaged using CLSM. As controls, one or more components of the above process were omitted.

ASSOCIATED CONTENT

Supporting Information

The Supporting Information is available free of charge at https://pubs.acs.org/doi/10.1021/jacsau.3c00803.

https://doi.org/10.1021/jacsau.3c00803
JACS Au 2024, 4, 828−836

Materials and methods, complete synthetic sequence, preparation of samples and testing process, and the corresponding charts associated with the manuscript. (DOCX)

AUTHOR INFORMATION

Corresponding Authors

Jianwei Jiao − *Medical Science and Technology Innovation Center, Shandong First Medical University, Jinan 250117, China; Laboratory of Stem Cell and Reproductive Biology, Institute of Zoology, Chinese Academy of Sciences, Beijing 100101, China*; Email: jwjiao@ioz.ac.cn

Yuna Guo − *Medical Science and Technology Innovation Center, Shandong First Medical University, Jinan 250117, China*; orcid.org/0009-0006-7828-0884; Email: gyn9901220@163.com

Authors

Gang Wang − *Medical Science and Technology Innovation Center, Shandong First Medical University, Jinan 250117, China; Nanjing University School of Life Sciences, Nanjing University, Nanjing 210023, China*

Ying Chen − *School of Clinical and Basic Medical Sciences, Shandong First Medical University, Jinan 250117, China*

Yuan Wei − *Medical Science and Technology Innovation Center, Shandong First Medical University, Jinan 250117, China*

Lei Zheng − *Medical Science and Technology Innovation Center, Shandong First Medical University, Jinan 250117, China*

Complete contact information is available at: https://pubs.acs.org/10.1021/jacsau.3c00803

Author Contributions

⊥G.W. and Y.C. contributed equally. All authors have given approval to the final version of the manuscript.

Notes

The authors declare no competing financial interest.

ACKNOWLEDGMENTS

This work received financial support from the National Natural Science Foundation of China (22304104), Shandong Provincial Natural Science Foundation (ZR2022QH260), and the Project for Scientific Research Innovation Team of Young Scholars in Colleges and Universities of Shandong Province (2022KJ196).

REFERENCES

(1) Geri, J. B.; Oakley, J. V.; Reyes-Robles, T.; Wang, T.; McCarver, S. J.; White, C. H.; Rodriguez-Rivera, F. P.; Parker, D. L., Jr; Hett, E. C.; Fadeyi, O. O.; Oslund, R. C.; MacMillan, D. W. C. Microenvironment mapping via dexter energy transfer on immune cells. *Science* **2020**, *367* (6482), 1091−1097.

(2) Senapati, S.; Das, S.; Batra, S. K. Mucin-interacting proteins: from function to therapeutics. *Trends Biochem. Sci.* **2010**, *35* (4), 236−245.

(3) Bose, M.; Mukherjee, P. Microbe−MUC1 crosstalk in cancer-associated infections. *Trends Mol. Med.* **2020**, *26* (3), 324−336.

(4) Nabavinia, M. S.; Gholoobi, A.; Charbgoo, F.; Nabavinia, M.; Ramezani, M.; Abnous, K. Anti-MUC1 aptamer: A potential opportunity for cancer treatment. *Med. Res. Rev.* **2017**, *37* (6), 1518−1539.

(5) Pochampalli, M. R.; Bitler, B. G.; Schroeder, J. A. Transforming growth factor α−dependent cancer progression is modulated by MUC1. *Cancer Res.* **2007**, *67* (14), 6591−6598.

(6) Ohyabu, N.; Kakiya, K.; Yokoi, Y.; Hinou, H.; Nishimura, S. I. Convergent solid-phase synthesis of macromolecular MUC1 models truly mimicking serum glycoprotein biomarkers of interstitial lung diseases. *J. Am. Chem. Soc.* **2016**, *138* (27), 8392−8395.

(7) Li, Y.; Huo, F.; Chen, L.; Wang, H.; Wu, J.; Zhang, P.; Feng, N.; Li, W.; Wang, L.; Wang, Y.; Wang, X.; Yang, X.; Lu, Z.; Mao, Y.; Yan, C.; Ding, L.; Ju, H. Protein-targeted glycan editing on living cells disrupts KRAS signaling. *Angew. Chem., Int. Ed.* **2023**, *62*, No. e202218148, DOI: 10.1002/anie.202218148.

(8) Yan, T.; Boatner, L. M.; Cui, L.; Tontonoz, P.; Backus, K. M. Defining the cell surface cysteinome using two-step enrichment proteomics. *JACS Au* **2023**, *3* (12), 3506−3523.

(9) Sachdeva, M.; Mo, Y. MicroRNA-145 suppresses cell invasion and metastasis by directly targeting mucin 1. *Cancer Res.* **2010**, *70* (1), 378−387.

(10) Wu, L.-L.; Wen, C.; Hu, J.; Tang, M.; Qi, C.; Li, N.; Liu, C.; Chen, L.; Pang, D.; Zhang, Z. Nanosphere-based one-step strategy for efficient and nondestructive detection of circulating tumor cells. *Biosens. Bioelectron.* **2017**, *94*, 219−226.

(11) Tan, W. C. C.; Nerurkar, S.; Cai, H.; Ng, H.; Wu, D.; Wee, Y.; Lim, J.; Yeong, J.; Lim, T. Overview of multiplex immunohistochemistry/immunofluorescence techniques in the era of cancer immunotherapy. *Cancer Commun.* **2020**, *40* (4), 135−153.

(12) Thul, P. J.; Åkesson, L.; Wiking, M.; Mahdessian, D.; Geladaki, A.; Blal, H. A.; Alm, T.; Asplund, A.; Björk, L.; Breckels, L. M.; Bäckström, A.; Danielsson, F.; Fagerberg, L.; Fall, J.; Gatto, L.; Gnann, C.; Hober, S.; Hjelmare, M.; Johansson, F.; Lee, S.; Lindskog, C.; Mulder, J.; Mulvey, C. M.; Nilsson, P.; Oksvold, P.; Rockberg, J.; Schutten, R.; Schwenk, J. M.; Sivertsson, A.; Sjöstedt, E.; Skogs, M.; Stadler, C.; Sullivan, D. P.; Tegel, H.; Winsnes, C.; Zhang, C.; Zwahlen, M.; Mardinoglu, A.; Pontén, F.; Feilitzen, K. V.; Lilley, K. S.; Uhlén, M.; Lundberg, E. A subcellular map of the human proteome. *Science* **2017**, *356* (6340), No. eaal3321.

(13) Wu, N.; Bao, L.; Ding, L.; Ju, H. A single excitation-duplexed imaging strategy for profiling cell surface protein-specific glycoforms. *Angew. Chem., Int. Ed.* **2016**, *55* (17), 5220−5224.

(14) Li, S.; Liu, Y.; Liu, L.; Feng, Y.; Ding, L.; Ju, H. A hierarchical coding strategy for live cell imaging of protein-specific glycoform. *Angew. Chem.* **2018**, *130* (37), 12183−12187.

(15) Meldal, M.; Diness, F. Recent fascinating aspects of the CuAAC click reaction. *Trends Chem.* **2020**, *2* (6), 569−584.

(16) Debets, M. F.; Tastan, O. Y.; Wisnovsky, S. P.; Malaker, S. A.; Angelis, N.; Moeckl, L. K. R.; Choi, J.; Flynn, H.; Wagner, L. J. S.; Bineva-Todd, G.; Antonopoulos, A.; Cioce, A.; Browne, W. M.; Li, Z.; Briggs, D. C.; Douglas, H. L.; Hess, G. T.; Agbay, A. J.; Roustan, C.; Kjaer, S.; Haslam, S. M.; Snijders, A. P.; Bassik, M. C.; Moerner, W. E.; Li, V. S. W.; Bertozzi, C. R.; Schumann, B. Metabolic precision labeling enables selective probing of *O*-linked *N*-acetylgalactosamine glycosylation. *Proc. Natl. Acad. Sci. U.S.A.* **2020**, *117* (41), 25293−25301.

(17) Sadler, J. C.; Brewster, R. C.; Kjeldsen, A.; González, A. F.; Nirkko, J. S.; Varzandeh, S.; Wallace, S. Overproduction of native and click-able colanic acid slime from engineered *Escherichia coli*. *JACS Au* **2023**, *3* (2), 378−383.

(18) Rhee, H. W.; Zou, P.; Udeshi, N. D.; Martell, J. D.; Mootha, V. K.; Carr, S. A.; Ting, A. Y. Proteomic mapping of mitochondria in living cells via spatially restricted enzymatic tagging. *Science* **2013**, *339* (6125), 1328−1331.

(19) Li, J.; Han, S.; Li, H.; Udeshi, N. D.; Svinkina, T.; Mani, D. R.; Xu, C.; Guajardo, R.; Xie, Q.; Li, T.; Luginbuhl, D. J.; Wu, B.; McLaughlin, C. N.; Xie, A.; Kaewsapsak, P.; Quake, S. R.; Carr, S. A.; Ting, A. Y.; Luo, L. Cell-surface proteomic profiling in the fly brain uncovers wiring regulators. *Cell* **2020**, *180*, 373−386.

(20) Zhao, X.; Suarez, J.; Khajo, A.; Yu, S.; Metlitsky, L.; Magliozzo, R. S. A radical on the Met-Tyr-Trp modification required for catalase activity in catalase-peroxidase is established by isotopic labeling and

site-directed mutagenesis. *J. Am. Chem. Soc.* **2010**, *132* (24), 8268−8269.
(21) Kotani, N.; Gu, J.; Isaji, T.; Udaka, K.; Taniguchi, N.; Honke, K. Biochemical visualization of cell surface molecular clustering in living cells. *Proc. Natl. Acad. Sci. U.S.A.* **2008**, *105* (21), 7405−7409.
(22) Li, L.; Xu, S.; Yan, H.; Li, X.; Yazd, H. S.; Li, X.; Huang, T.; Cui, C.; Jiang, J.; Tan, W. Nucleic acid aptamers for molecular diagnostics and therapeutics: advances and perspectives. *Angew. Chem., Int. Ed.* **2021**, *60* (5), 2221−2231.
(23) Tanaka, K.; Okuda, T.; Kasahara, Y.; Obika, S. Base-modified aptamers obtained by cell-internalization SELEX facilitate cellular uptake of an antisense oligonucleotide. *Mol. Ther. Nucleic Acids* **2021**, *23*, 440−449.
(24) Zhu, G.; Chen, X. Aptamer-based targeted therapy. *Adv. Drug Delivery Rev.* **2018**, *134*, 65−78.
(25) Guo, Y.; Wang, P.; Jiang, L.; Deng, C.; Zheng, L.; Song, C.; Jiao, J. Multifunctional proximity labeling strategy for lipid raft-specific sialic acid tracking and engineering. *Bioconjugate Chem.* **2023**, *34* (10), 1719−1726.
(26) Guo, Y.; Wang, N.; Zhong, Y.; Li, W.; Li, Y.; Wang, G.; Yao, Y.; Shi, Y.; Chen, L.; Wang, X.; Ding, L.; Ju, H. Cell-selective multifunctional surface covalent reconfiguration using aptamer enabled proximity catalytic labeling. *J. Am. Chem. Soc.* **2023**, *145* (9), 5092−5104.
(27) Ferreira, C. S. M.; Matthews, C. S.; Missailidis, S. DNA aptamers that bind to MUC1 tumour marker: design and characterization of MUC1-binding single-stranded DNA aptamers. *Tumor Biol.* **2006**, *27* (6), 289−301.
(28) Fan, C.; Shi, J.; Zhuang, Y.; Zhang, L.; Huang, L.; Yang, W.; Chen, B.; Chen, Y.; Xiao, Z.; Shen, H.; Zhao, Y.; Dai, J. Myocardial-infarction-responsive smart hydrogels targeting matrix metalloproteinase for on-demand growth factor delivery. *Adv. Mater.* **2019**, *31* (40), No. 1902900.
(29) Gao, X.; Sun, Z.; Wang, X.; Zhang, W.; Xu, D.; Sun, X.; Guo, Y.; Xu, S.; Li, F. Construction of a dual-model aptasensor based on G-quadruplexes generated via rolling circle amplification for visual/sensitive detection of kanamycin. *Sci. Total Environ.* **2022**, *839*, No. 156276.
(30) Jeong, J. H.; Schmidt, J. J.; Kohman, R. E.; Zill, A. T.; DeVolder, R. J.; Smith, C. E.; Lai, M.-H.; Shkumatov, A.; Jensen, T. W.; Schook, L. G.; Zimmerman, S. C.; Kong, H. Leukocyte-mimicking stem cell delivery via in situ coating of cells with a bioactive hyperbranched polyglycerol. *J. Am. Chem. Soc.* **2013**, *135* (24), 8770−8773.
(31) Barrett, R. M.; Liu, H. W.; Jin, H.; Goodman, R. H.; Cohen, M. S. Cell-specific profiling of nascent proteomes using orthogonal enzyme-mediated puromycin incorporation. *ACS Chem. Biol.* **2016**, *11* (6), 1532−1536.
(32) Zhang, D.; Zheng, Y.; Lin, Z.; Liu, X.; Li, J.; Yang, H.; Tan, W. Equipping natural killer cells with specific targeting and checkpoint blocking aptamers for enhanced adoptive immunotherapy in solid tumors. *Angew. Chem., Int. Ed.* **2020**, *59*, 12022−12028.
(33) Li, J.; Xun, K.; Zheng, L.; Peng, X.; Qiu, L.; Tan, W. DNA-based dynamic mimicry of membrane proteins for programming adaptive cellular interactions. *J. Am. Chem. Soc.* **2021**, *143* (12), 4585−4592.
(34) Yasumizu, Y.; Rajabi, H.; Jin, C.; Hata, T.; Pitroda, S.; Long, M. D.; Hagiwara, M.; Li, W.; Hu, Q.; Liu, S.; Yamashita, N.; Fushimi, A.; Kui, L.; Samur, M.; Yamamoto, M.; Zhang, Y.; Zhang, N.; Hong, D.; Maeda, T.; Kosaka, T.; Wong, K. K.; Oya, M.; Kufe, D. MUC1-C regulates lineage plasticity driving progression to neuroendocrine prostate cancer. *Nat. Commun.* **2020**, *11* (1), No. 338.
(35) Minopoli, A.; Della Ventura, B.; Lenyk, B.; Gentile, F.; Tanner, J. A.; Offenhäusser, A.; Mayer, D.; Velotta, R. Ultrasensitive antibody-aptamer plasmonic biosensor for malaria biomarker detection in whole blood. *Nat. Commun.* **2020**, *11* (1), No. 6134.
(36) Schjoldager, K. T.; Narimatsu, Y.; Joshi, H. J.; Clausen, H. Global view of human protein glycosylation pathways and functions. *Nat. Rev. Mol. Cell Biol.* **2020**, *21* (12), 729−749.
(37) Sun, R.; Kim, A. M. J.; Lim, S. O. Glycosylation of immune receptors in cancer. *Cells* **2021**, *10* (5), 1100.
(38) Mattey, A. P.; Birmingham, W. R.; Both, P.; Kress, N.; Huang, K.; Van Munster, J. M.; Bulmer, G. S.; Parmeggiani, F.; Voglmeir, J.; Martinez, J. E. R.; Turner, N. J.; Flitsch, S. L. Selective oxidation of *N*-glycolylneuraminic acid using an engineered galactose oxidase variant. *ACS Catal.* **2019**, *9* (9), 8208−8212.

https://doi.org/10.1021/jacsau.3c00803
JACS Au 2024, 4, 828−836